ACS APPLIED MATERIALS & INTERFACES

Research Article

www.acsami.org

Reducing Adhesion Force by Means of Atomic Layer Deposition of ZnO Films with Nanoscale Surface Roughness

Zhimin Chai,[†] Yuhong Liu,[†] Xinchun Lu,*[,†] and Dannong He[‡]

[†]The State Key Laboratory of Tribology, Tsinghua University, Beijing 100084, People's Republic of China

[‡]National Engineering Research Center for Nanotechnology and Application, Shanghai 200241, People's Republic of China

Supporting Information

ABSTRACT: Adhesion is a big concern for the design of Si-based microelectromechanical devices. A ZnO film with nanoscale surface roughness is a promising candidate to decrease adhesion as the protective coating. In this study, the adhesion force of ZnO films prepared by atomic layer deposition (ALD) on a Si (100) substrate was studied. The root-mean-square (RMS) roughness of the ZnO films was in the range of 0.7−4.28 nm, and the contact angle of water was in the range of 85−88°. The adhesion force was measured by atomic force microscopy (AFM) at both low (12%) and high (60%) relative humidities. The results show that the adhesion force decreases as the surface roughness increases. A low adhesion force at high RMS roughness is attributed to the large asperities on the film, and a large adhesion force at high humidity is attributed to the large capillary force. The experimental adhesion force was compared to the force calculated using the Rabinovich model. Although the theoretical value underestimates the experimental value, the proportion of the two components of the adhesion force is clearly shown. At the low humidity, the van der Waals force component differs not greatly with the capillary force component, while at the high humidity, the capillary force component becomes dominant.

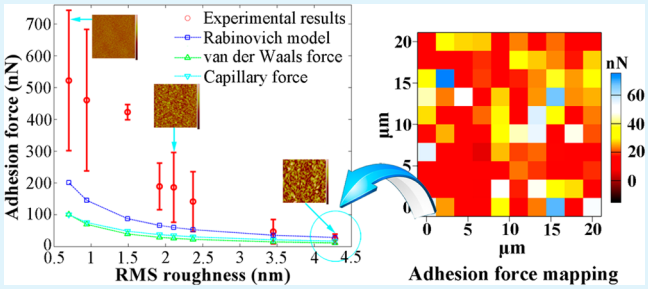

KEYWORDS: *adhesion force, nanascale, surface roughness, ALD, ZnO*

INTRODUCTION

Microelectromechanical system (MEMS) devices, including gyroscopes, accelerometers, radio frequency (RF) switches, inertial sensors, and temperature/humidity sensors, have been increasingly used in mobile devices, such as cell phones and tablets.[1] The widespread application of these MEMS devices is attributed to the absence of contacting parts. However, for many exciting applications, such as micro gears and motors, contacting and rubbing structures are inevitable.[2,3] Adhesion force may make the contacting structures adhere to each other, which restricts the reliable running of the devices. To ensure the normal operation of these devices, adhesion force should be taken into consideration. Various forces, such as capillary, van der Waals, and electrostatic forces contribute to the adhesion force.[4] With reduction of one or more forces, the adhesion force can be reduced.

Silicon (Si) material, usually used to fabricate MEMS devices, is hydrophilic in nature, which induces a large capillary force. The most conventional way to reduce the capillary force is to coat the Si surface with hydrophobic films. It was demonstrated that various films, such as self-assembled monolayers (SAMs)[5−8] and Al_2O_3,[9] can efficiently increase hydrophobicity and reduce the capillary force. Wurtzite-type ZnO is also a prospective material for the hydrophobic films because of its excellent hydrophobic property.[10−13] Surface roughening is another way to reduce adhesion force. Large surface roughness reduces the contact area between two contacting bodies, which, in turn, decreases the van der Waals force.[14−21] In conclusion, if a ZnO film with nanoscale surface roughness is prepared on the surface of Si-based MEMS devices, the adhesion force of the devices can be decreased.

ZnO films used in our study were prepared by an atomic layer deposition (ALD) technique.[22] In comparison to other techniques, such as sputtering deposition (SP), ion beam deposition (IBD), pulsed laser deposition (PLD), and chemical vapor deposition (CVD), the ALD technique excels in the aspect that the films deposited have unique conformality.[23,24] This is vital for MEMS devices, because in these devices, complicated three-dimensional (3D) and shadowed structures are common. It has been demonstrated that both the exposed and shadowed surfaces of the MEMS devices can be conformally coated with ALD films.[25] ZnO films prepared by ALD are usually polycrystalline in nature.[26,27] By adjusting the grain size of the ZnO films, surfaces with various roughnesses can be obtained.

In our study, the adhesion force of ZnO films with nanoscale surface roughness was investigated. The ZnO films with various film thicknesses were deposited on the Si (100) substrate. As

Received: November 25, 2013
Accepted: February 7, 2014
Published: February 7, 2014

the grain size of the ZnO film increases with film thickness, the surface roughness increases correspondingly. The adhesion force was measured by atomic force microscopy (AFM) at relative humidities of 12 and 60%, and the result was compared to the Rabinovich model.

EXPERIMENTAL SECTION

Sample Preparation. Polycrystalline ZnO films with different root-mean-square (RMS) roughness were prepared by ALD using a Picosun SUNALE R-150 reactor. The detailed deposition process has been described elsewhere.[26] ZnO films were deposited on the Si (100) substrate, and the substrate temperature was 150 °C. Films with different surface geometries were prepared by adjusting the film thickness. A total of 50−1000 ALD cycles were conducted to obtain ZnO films with a thickness in the range of 10.0−182.1 nm.

Tapping mode AFM (Veeco) was used to obtain the surface morphology of the films. The probe used was PPP-NCHR-20 (NanoSensors) with a spring constant of ~42 N/m and resonant frequency of ~300 kHz in the ambient air. Roughness in terms of RMS was subsequently determined by the off-line analysis software.

The hydrophobic characteristics of ZnO films were studied by the static contact angle measurement. The contact angles were measured by a homemade contact angle analyzer, whose basic principle was similar to that from Kwok and Neumann.[28] The droplet volume was about 10 μL. For each sample, four different readings were recorded minimally with the typical error of about 2°.

Adhesion Force. The adhesion force was measured experimentally by AFM (MFP3D, Asylum Research) in the force calibration mode.[29] The measurement was conducted in both low (12 ± 2%) and high (60 ± 5%) relative humidities. The ambient temperature was 26 ± 0.5 °C. Prior to the acquisition of the force curve, a 20 × 20 μm^2 topography image was obtained in a contact mode to obtain the desired location. The normal load applied on the sample was 73.9 nN, which was low enough to avoid the damage of the sample. Once the interested area was located, the scanner was stopped and the tip was positioned in the scan area to make indentations. To obtain sufficient statistics, a 10 × 10 indentation matrix was obtained for each sample. Moreover, such a matrix was repeatedly measured in three locations on the surface. For each indentation, a force curve was recorded, from which the adhesion force can be extracted. When a Gaussian distribution was fitted, the mean and standard deviation of the adhesion force were calculated. Adhesion force values that were more than 2 standard deviations away from the average value were rejected.

A homemade colloidal probe was used in our experiment. Because the adhesion force measured by the colloidal probe is usually large, the result can be more sensitive.[30] The probe was made by gluing a silica microsphere (Nano-Micro Technology Company) to a tipless cantilever (AIOAl-TL, BudgetSensors) with HI-TOP 3136 UV glue (HI-TOP Fine Chemical Co., Ltd.). The spring constant of the cantilever was 1.86 N/nm, and the nominal diameter of the sphere was 10 μm, which was larger than 8.85 μm measured from the scanning electron microscopy (SEM, FEI Quanta 200 FEG) image (see Figure 1S of the Supporting Information). The probe was also characterized by scanning a calibration grating TGT01 (Mikromasch),[31] and the radius of the sphere obtained was 4.35 ± 0.25 μm, which was consistent with that obtained by the SEM image (as detailed in the Supporting Information).

RESULTS AND DISCUSSION

Film Properties. Figure 1 shows the AFM images of ZnO films with various film thicknesses. It can be seen that, at the initial period of deposition (Figure 1a, with a film thickness of 10.0 nm), the grain of the polycrystalline ZnO film is small (~10 nm) and in a round shape. With the growth of the ZnO film, the grain size increases. However, the round shape of the grain is retained. As the film thickness exceeds 91.1 nm, the grain becomes longish. This may be due to the coalescence of adjacent grains. The increase of the grain sizewith film thickness results in the growth of RMS roughness, as shown in Figure 2. The roughness value of ZnO films is in the range of 0.70−4.28 nm, while the RMS roughness of the Si substrate is only 0.35 nm. The nanoscale rough surface was used to investigate the effect of roughness on adhesion force.

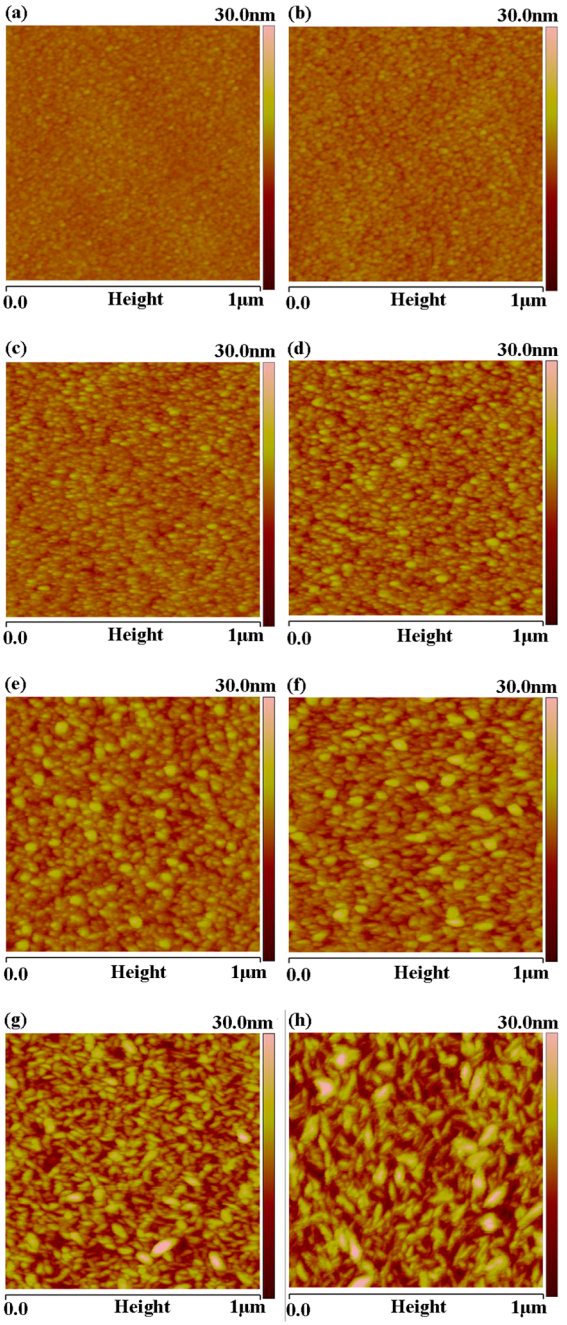

Figure 1. Surface morphologies of ZnO films with thicknesses of (a) 10.0 nm, (b) 19.2 nm, (c) 36.7 nm, (d) 54.3 nm, (e) 72.4 nm, (f) 91.1 nm, (g) 132.3 nm, and (h) 182.1 nm.

Because the capillary force contributes to adhesion greatly, the wetting ability of the surface should be studied before the measurement of the adhesion force. Figure 3a shows a drop of water on the 10.0 nm thick ZnO film. The contact angle is 87.9°; thus, the surface is almost hydrophobic. The contact angles of ZnO films change little as the film thickness increases, as shown in Figure 3b. A large contact angle of ~90° is likely

dx.doi.org/10.1021/am4053333 | ACS Appl. Mater. Interfaces 2014, 6, 3325−3330

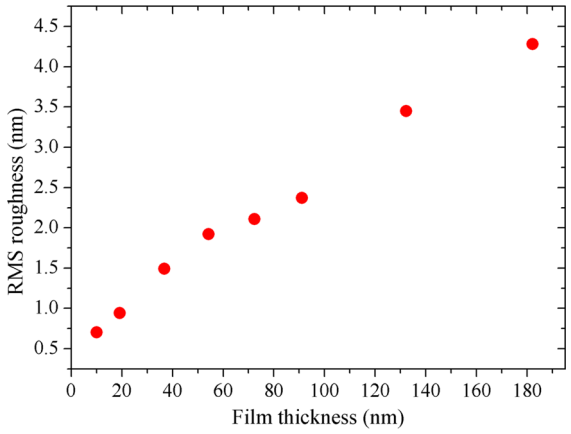

Figure 2. RMS roughness of various ZnO films as a function of film thickness.

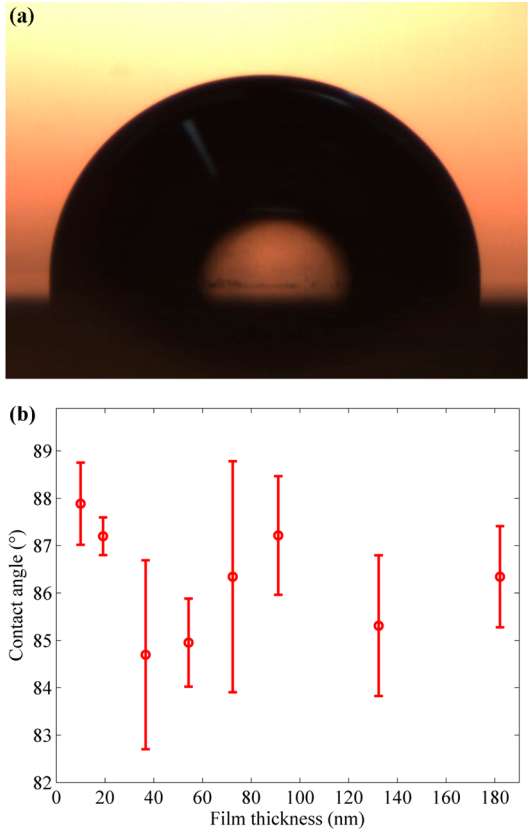

Figure 3. (a) Water droplet on the 10.0 nm thick ZnO film. (b) Contact angles of ZnO films with various film thicknesses.

due to the small surface energy of ZnO.[11] The surface energy of the ZnO film extracted from the Owens and Wendt approach[32] is 33 mJ/m^2, which is smaller than 40−52 mJ/m^2 of Si (coated with a thin layer of native oxide).[33]

Adhesion Force. The value of the adhesion force is measured from the interaction of the AFM tip with the sample surface. Figure 4 shows four common configurations of tip−sample interaction: (a) AFM tip interacts with large asperities on the surface; (b) AFM tip interacts with small asperities; (c) AFM tip interacts with the area between two adjacent asperities; and (d) AFM tip interacts with the area between two adjacent asperities, which possess larger spacing. Because the asperity with a larger radius reduces real contact area,[17] the

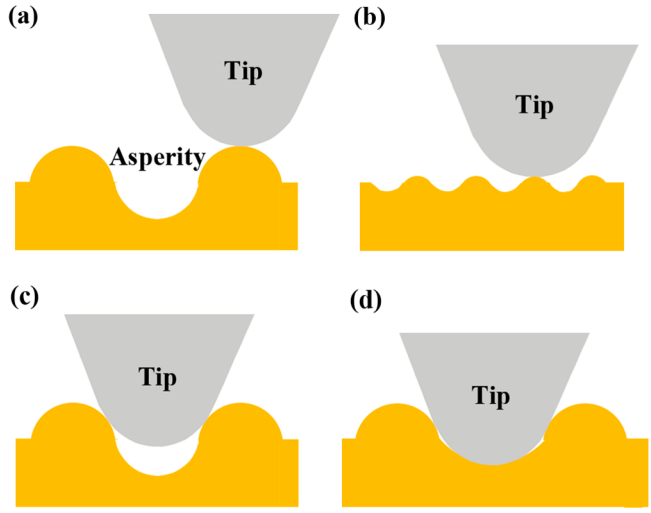

Figure 4. Schematic showing the tip−sample interaction: (a) AFM tip interacts with big asperities on the surface; (b) AFM tip interacts with small asperities; (c) AFM tip interacts with the area between two adjacent asperities; and (d) AFM tip interacts with the area between two adjacent asperities, which possess larger spacing.

adhesion force obtained from configuration a can be smaller than that from configuration b. In addition, the separation distance between the tip and substrate is large for configuration a, which further decreases the adhesion force. For configuration c, the tip not only contacts the asperity but also the area between two asperities. Because the spacing of two asperities is smaller than the tip radius, the tip does not contact the substrate. Thus, the interaction between the tip and substrate can be ignored. However, the adhesion force obtained from this configuration is still larger than that obtained from the condition of configuration a because two asperities contact the tip simultaneously. The spacing of adjacent asperities increases for configuration d. In configuration d, the interaction from the substrate should be concerned. Accordingly, the adhesion force is larger than that obtained from configuration c.

Adhesion Force Measured by AFM. Adhesion force between the colloidal probe and the ZnO film was measured by AFM in an area of 20 × 20 μm^2. Figure 5a shows the adhesion force map of the ZnO film with RMS roughness of 4.28 nm measured at the relative humidity of 12%. The force values are represented by colors, with a blue color for a high adhesion force and a dark color for a small force. A total of 100 force values can be obtained from this mapping.

The adhesion force histogram is presented in Figure 5b. It can be seen that the distribution of the adhesion force is rather broad. Because the radii and spacing of asperities are stochastic for the ZnO film, the contact status of the tip and sample may be one of the four configurations discussed above. Therefore, the adhesion force shows high standard deviation. Besides, the distribution of the adhesion force shows high asymmetry. The mean and standard deviation of the adhesion force were calculated by fitting to a Gausssian distribution, as shown in Figure 5b.

Figure 6a shows the experimentally measured adhesion force between the colloidal probe and the ZnO film at the relative humidity of 12%. For all of the ZnO films, a large standard deviation for the adhesion force is observed. The adhesion force decreases gradually with an increasing surface roughness. The lowest adhesion force for the rough surface (RMS roughness of

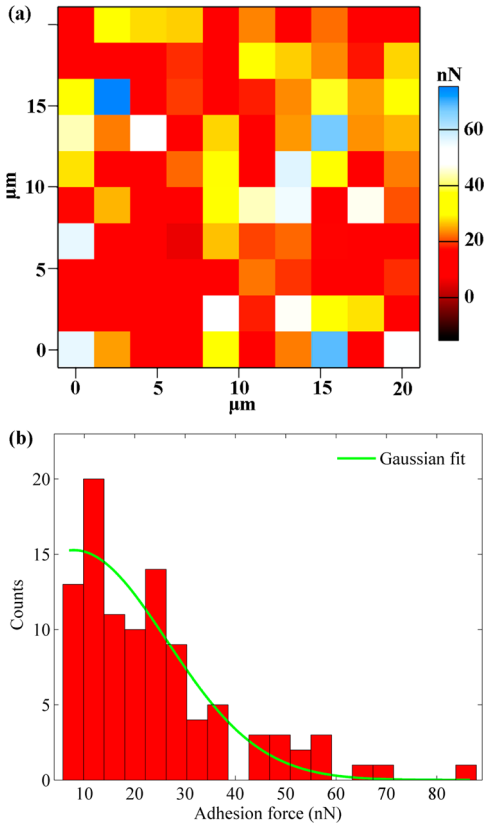

Figure 5. (a) Adhesion force map of the ZnO film with a roughness of 4.28 nm obtained using the colloidal probe at the relative humidity of 12%. A total of 100 adhesion forces can be obtained from this map. (b) Distribution of adhesion forces. The green line is the Gaussian fit to this distribution, from which the mean and standard deviation of the adhesion force can be calculated.

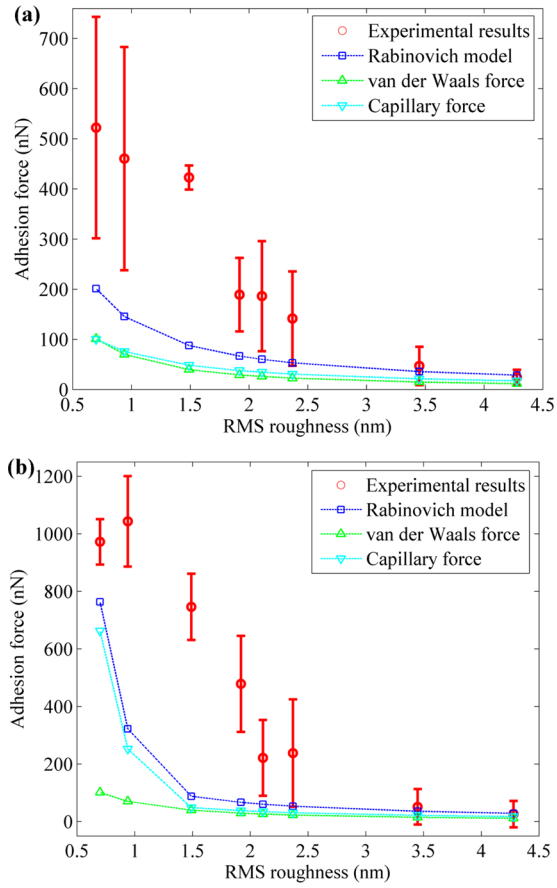

Figure 6. Adhesion force between the colloidal probe and the ZnO film as a function of RMS roughness measured at relative humidities of (a) 12% and (b) 60%. The blue dashed line represents the adhesion force calculated using the Rabinovich model; the green dashed line represents the van der Waals force component; and the cyan dashed line represents the capillary force component.

4.8 nm) is attributed to the large asperities on the surface of the film. Because the contact between the colloidal tip and the film mainly occurs on these large asperities, the real area of contact is lowered significantly, which decreases the adhesion force.

Figure 6b shows the adhesion force between the colloidal probe and the ZnO film measured at the relative humidity of 60%. As with the low humidity of 12%, a tendency that the adhesion force decreases as the surface roughness increases is observed. However, the adhesion force value measured at high humidity is higher than that measured at low humidity. A large adhesion force at high humidity is due to the large capillary force, which will be discussed in the next section.

Comparison to the Rabinovich Model. In this section, the measured adhesion force was compared to the Rabinovich model.[34−37] Figure 7 shows the schematic illustration of the Rabinovich model. In this model, the asperity on the ZnO film surface is approximated by a hemisphere. The tip contacts a single asperity perpendicularly along a line connecting their centers. The minimum separation between the tip and the asperity is H_0, which is approximately 0.3 nm. In the humidity environment, a condensed water layer exists between the contacting surfaces as a capillary bridge.

In the Rabinovich model, adhesion force consists of two parts: the van der Waals force and the capillary force. The van der Waals force is calculated by

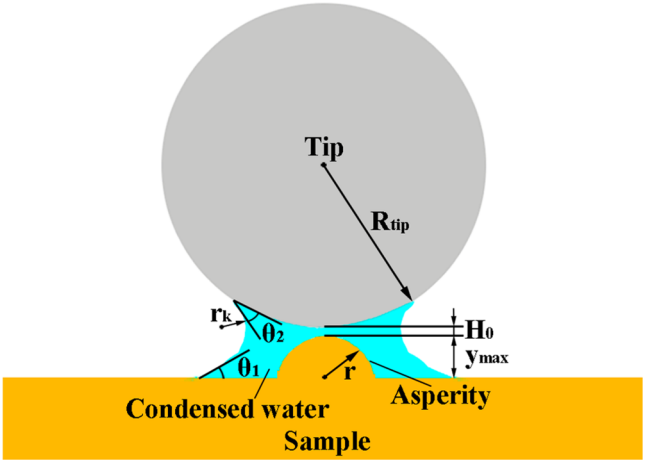

Figure 7. Schematic illustration of the Rabinovich model.

$$F_{vdw} = \frac{A_H R_{tip}}{6H_0^2}\left[\frac{r}{r + R_{tip}} + \frac{1}{(1 + y_{max}/H_0)^2}\right] \quad (1)$$

where A_H is the Hamaker constant, R_{tip} is the radius of the tip, r is the radius of the asperity, and y_{max} is the maximum value of the asperity height. The radius of the asperity is obtained by

dx.doi.org/10.1021/am4053333 | ACS Appl. Mater. Interfaces 2014, 6, 3325−3330

$$r = \frac{\lambda^2}{58\text{rms}} \tag{2}$$

and the height of the asperity is obtained by

$$y_{\max} = 1.817\text{rms} \tag{3}$$

where λ is the distance between two adjacent asperities, and rms is the roughness value of the ZnO film surface. The van der Waals force contains two terms: the first term resulting from the contact between the tip and the asperity and the second term resulting from the non-contact interaction between the tip and the substrate.

The capillary force is calculated by

$$F_c = 4\pi\gamma_L R_{tip} \cos\theta\left[1 - \frac{H}{2r_k \cos\theta}\right], \quad \text{if } H \le 2r_k \cos\theta$$
$$F_c = 4\pi\gamma_L R_{eff} \cos\theta, \quad \text{if } H > 2r_k \cos\theta \tag{4}$$

where γ_L is the surface tension of water, θ is the contact angle of water, $H = H_0 + y_{\max}$ is the distance between the surface plane and the bottom of the tip, $R_{eff} = R_{tip}r/(R_{tip} + r)$ is the effective radius, and r_k is the equilibrium radius of the meniscus

$$\cos\theta = \frac{\cos\theta_1 + \cos\theta_2}{2} \tag{5}$$

where θ_1 is the contact angle of water on the ZnO film surface and θ_2 is the contact angle of water on the tip surface.

The total adhesion force is obtained by

$$F_a = F_{vdw} + F_c \tag{6}$$

With this model, the relation between the adhesion force and roughness is established.

To calculate the adhesion force, the values of a large amount of parameters should be determined. For the Hamaker constant between two different materials, a combining rule approximation is used

$$A_{H12} = \sqrt{A_{H11}A_{H22}} \tag{7}$$

where A_{H11} and A_{H22} are the Hamaker constants of each material. Another parameter that should be determined is the asperity−asperity distance λ, which is measured from the surface morphology. Because the selection of asperity is arbitrary, the value of λ is more indicative than absolute. An approximate value of 100 nm is chosen for this distance. Detailed input values for the Rabinovich model are shown in Table 1.

Table 1. Input Values for the Rabinovich Model

parameter	value
A_{H_ZnO} (J)	2.65×10^{-19} [a]
A_{H_tip} (J)	0.65×10^{-19} [a]
R_{tip} (μm)	4.35 ± 0.25
H_0 (nm)	0.3
γ_L (mN/m)	72.8
θ_{tip} (deg)	30[b]
r_k (nm)	0.54 and 2.43 (at the relative humidities of 12 and 60%, respectively)[c]

[a]From ref 35. [b]From ref 38. [c]Calculated from the inline equation in ref 39.

The blue dashed line presented in Figure 6 is the adhesion force calculated using the Rabinovich model; the green dashed line is the van der Waals force component; and the cyan dashed line is the capillary force component.

Because the van der Waals force is independent with the humidity, the force value is the same for both the low (12%) and high (60%) humidities. With the increase of surface roughness, the real contact area decreases. Accordingly, the van der Waals force decreases. Contrary to the van der Waals force, the capillary force is strongly influenced by the humidity. When the humidity increases from 12 to 60%, the equilibrium radius of the meniscus (r_k) increases from 0.54 to 2.43 nm. More water condenses between the tip and film surface, and thus, the capillary force increases. The size of the meniscus is also influenced by the surface roughness. With the increase of surface roughness, the size of the meniscus decreases and the capillary force decreases correspondingly. It can be observed that, at the relative humidity of 60%, the capillary force decreases by 1 order of magnitude as the surface roughness increases from 0.70 to 4.28 nm.

At the low humidity of 12%, the values of the van der Waals force and the capillary force differ not greatly, while at the high humidity of 60%, the capillary force becomes dominated, especially when the surface roughness is small.

The total adhesion force is the sum of the van der Waals force and the capillary force. A tendency that the adhesion force decreases as the surface roughness increases is observed for both the experimental and theoretical methods. However, the theoretical value underestimates the experimental value. This may be caused by the fact that only a single asperity contact is considered in this model. To achieve a more accurate estimation, multiple contacts should be taken into account.[40]

CONCLUSION

In our study, the adhesion force between the AFM tip and ZnO film prepared by ALD was studied. The surface of the ZnO film has nanoscale roughness and is almost hydrophobic. Because of the stochastic nature of asperity distribution on the film surface, the measured adhesion force shows high standard deviation. For both low (12%) and high (60%) relative humidities, a decrease of the adhesion force as a function of RMS roughness is observed. A low adhesion force at high roughness is due to the large asperities on the film surface. The adhesion force value measured at high humidity is higher than that measured at low humidity. A large adhesion force at high humidity is due to a large capillary force. We compared our experiments to the Rabinovich model, and the result reveals that the theoretical value underestimates the experimental value. Even so, the percentage of the van der Waals force and the capillary force in total adhesion force is clearly shown in the theoretical model. At the low humidity, the values of the van der Waals force and the capillary force do not differ greatly, while at the high humidity, the capillary force becomes dominant.

ASSOCIATED CONTENT

Supporting Information

SEM image of the colloidal probe (Figure 1S), AFM image of the colloidal probe (Figure 2S), and calculation of the tip radius using eq 1S. This material is available free of charge via the Internet at http://pubs.acs.org.

AUTHOR INFORMATION

Corresponding Author

*Telephone/Fax: +86-10-6279-7362. E-mail: xclu@tsinghua.edu.cn.

Notes

The authors declare no competing financial interest.

ACKNOWLEDGMENTS

The authors greatly appreciate the financial support of the National Science Fund for Distinguished Young Scholars (50825501), the Science Fund for Creative Research Groups (51321092), the National Natural Science Foundation of China (51335005), and the National Science and Technology Major Project (2008ZX02104-001). Helpful discussions with Wen Jing are gratefully acknowledged.

REFERENCES

(1) Yole Développement Company. http://www.yole.fr (accessed Sept 12, 2013).

(2) Kim, S. H.; Asay, D. B.; Dugger, M. T. *Nano Today* **2007**, *2*, 22−29.

(3) Williams, J. A.; Le, H. R. *J. Phys. D: Appl. Phys.* **2006**, *39*, R201−R214.

(4) Maboudian, R.; Howe, R. T. *J. Vac. Sci. Technol., B: Microelectron. Nanometer Struct.—Process., Meas., Phenom.* **1997**, *15*, 1−20.

(5) Mayer, T. M.; de Boer, M. P.; Shinn, N. D.; Clews, P. J.; Michalske, T. A. *J. Vac. Sci. Technol., B: Microelectron. Nanometer Struct.—Process., Meas., Phenom.* **2000**, *18*, 2433−2440.

(6) Maboudian, R.; Ashurst, W. R.; Carraro, C. *Sens. Actuators* **2000**, *82*, 219−223.

(7) Penskiy, I.; Gerratt, A. P.; Bergbreiter, S. *J. Micromech. Microeng.* **2011**, *21*, 105013.

(8) Xiang, H.; Komvopoulos, K. *J. Appl. Phys.* **2013**, *113*, 224505.

(9) Hoivik, N.; Elam, J.; Linderman, R.; Bright, V. M.; George, S.; Lee, Y. C. Atomic layer deposition of conformal dielectric and protective coatings for released micro-electromechanical devices. *Proceedings of the 15th IEEE International Conference on Micro Electro Mechanical Systems*; Las Vegas, NV, Jan 20−24, 2002; pp 455−458.

(10) Kumar, P. S.; Raj, A. D.; Mangalaraj, D.; Nataraj, D. *Thin Solid Films* **2010**, *518*, E183−E186.

(11) Sheng, Y.; Yiting, W.; Xiangyu, Z.; Jia, Z. Fabrication and analysis of super-hydrophobic ZnO film for microfluidic devices. *Proceedings of the 10th IEEE International Conference on Solid-State and Integrated Circuit Technology*; Shanghai, China, Nov 1−4, 2010.

(12) Ma, K.; Li, H.; Zhang, H.; Xu, X. L.; Gong, M. G.; Yang, Z. *Chin. Phys. B* **2009**, *18*, 1942−1946.

(13) Shinde, V. R.; Lokhande, C. D.; Mane, R. S.; Han, S. H. *Appl. Surf. Sci.* **2005**, *245*, 407−413.

(14) Liu, D. L.; Martin, J.; Burnham, N. A. *Appl. Phys. Lett.* **2007**, *91*, 043107.

(15) Zheng, W.; Mengfu, H.; Yapu, Z. *J. Adhes. Sci. Technol.* **2010**, *24*, 1045−1054.

(16) Ramakrishna, S. N.; Clasohm, L. Y.; Rao, A.; Spencer, N. D. *Langmuir* **2011**, *27*, 9972−9978.

(17) Zhang, X. L.; Lu, Y. J.; Liu, E. Y.; Yi, G. W.; Jia, J. H. *Colloids Surf., A* **2012**, *401*, 90−96.

(18) Colak, A.; Wormeester, H.; Zandvliet, H.; Poelsema, B. *Appl. Surf. Sci.* **2012**, *258*, 6938−6942.

(19) Fischer, H. R.; Gelinck, E. *Appl. Surf. Sci.* **2012**, *258*, 9011−9017.

(20) Dejeu, J.; Bechelany, M.; Philippe, L.; Rougeot, P.; Michler, J.; Gauthier, M. *ACS Appl. Mater. Interfaces* **2010**, *2*, 1630−1636.

(21) Sherman, S. D.; Quist, A.; Hansma, P. *J. Nano Res.* **2009**, *6*, 225−235.

(22) George, S. M. *Chem. Rev.* **2010**, *110*, 111−131.

(23) Leskela, M.; Ritala, M. *Angew. Chem., Int. Ed.* **2003**, *42*, 5548−5554.

(24) Leskela, M.; Ritala, M. *Thin Solid Films* **2002**, *409*, 138−146.

(25) Mayer, T. M.; Elam, J. W.; George, S. M.; Kotula, P. G.; Goeke, R. S. *Appl. Phys. Lett.* **2003**, *82*, 2883−2885.

(26) Chai, Z. M.; Lu, X. C.; He, D. N. *Surf. Coat. Technol.* **2012**, *207*, 361−366.

(27) Wojcik, A.; Godlewski, M.; Guziewicz, E.; Minikayev, R.; Paszkowicz, W. *J. Cryst. Growth* **2008**, *310*, 284−289.

(28) Kwok, D. Y.; Neumann, A. W. *Adv. Colloid Interface Sci.* **1999**, *81*, 167−249.

(29) Bhushan, B.; Sundararajan, S. *Acta Mater.* **1998**, *46*, 3793−3804.

(30) Butt, H. J.; Cappella, B.; Kappl, M. *Surf. Sci. Rep.* **2005**, *59*, 1−152.

(31) Neto, C.; Craig, V. *Langmuir* **2001**, *17*, 2097−2099.

(32) Owens, D. K.; Wendt, R. C. *J. Appl. Polym. Sci.* **1969**, *13*, 1741−1747.

(33) Miskiewicz, P.; Kotarba, S.; Jung, J.; Marszalek, T.; Mas-Torrent, M.; Gomar-Nadal, E.; Amabilino, D. B.; Rovira, C.; Veciana, J.; Maniukiewicz, W.; Ulanski, J. *J. Appl. Phys.* **2008**, *104*, 054509.

(34) Rabinovich, Y. I.; Adler, J. J.; Ata, A.; Singh, R. K.; Moudgil, B. M. *J. Colloid Interface Sci.* **2000**, *232*, 10−16.

(35) Rabinovich, Y. I.; Adler, J. J.; Ata, A.; Singh, R. K.; Moudgil, B. M.; Abbas, M. *J. Colloid Interface Sci.* **2000**, *232*, 17−24.

(36) Rabinovich, Y. I.; Adler, J. J.; Esayanur, M. S.; Ata, A.; Singh, R. K.; Moudgil, B. M. *Adv. Colloid Interface Sci.* **2002**, *96*, 213−230.

(37) Ata, A.; Rabinovich, Y. I.; Singh, R. K. *J. Adhes. Sci. Technol.* **2002**, *16*, 337−346.

(38) Sung, M. M.; Kluth, G. J.; Maboudian, R. *J. Vac. Sci. Technol., A* **1999**, *17*, 540−544.

(39) van Zwol, P. J.; Palasantzas, G.; De Hosson, J. *Phys. Rev. E: Stat., Nonlinear, Soft Matter Phys.* **2008**, *78*, 031606.

(40) Katainen, J.; Paajanen, M.; Ahtola, E.; Pore, V.; Lahtinen, J. *J. Colloid Interface Sci.* **2006**, *304*, 524−529.